❏ 1746

Design and modeling of solenoid inductor integrated with FeNiCo in high frequency

Abdelhadi Namoune[1], Rachid Taleb[2], Noureddine Mansour[3]
[1]Electrical Engineering Department, Institute of Sciences and Technology, Ahmed Zabana University Centre, Algeria
[2]Electrical Engineering Department, Hassiba Benbouali University, Algeria
[2]Laboratoire Génie Electrique et Energies Renouvelables (LGEER), Algeria
[3]College of Engineering, University of Bahrain, Bahrain

Article Info

ABSTRACT

In this work, the design and modeling of the solenoid inductor are discussed. The layout of integrated inductors with magnetic cores and their geometrical parameters are developed. The quality factor Q and inductance value L are derived from the S-parameters and plotted versus frequency. The effect of solenoid inductor geometry on inductance and quality factor are studied via simulation using MATLAB. The solenoid inductor geometry parameters considered are the turn's number, the magnetic core length, the width of a magnetic core, the gap between turns, the magnetic core thickness, the coil thickness, and solenoid inductor oxide thickness. The performance of the proposed solenoid inductor integrated with FeNiCo is compared with other solenoid inductors.

Corresponding Author:

Abdelhadi Namoune,
Electrical Engineering Department,
Institute of Sciences and Technology,
Ahmed Zabana University Centre, Relizane, Algeria.
Email: namoune.abdelhadi@gmail.com

1. INTRODUCTION

The high demand for decreasing the size and weight of communication devices has been a strong incentive for researchers to improve monolithic inductors [1, 2]. The inductor is the least compatible passive device with silicon integration and subsequent scaling [3] and is often used in RF (radio frequencies) applications as a discrete device rather than an integrated circuit into the silicon chip [4]. The bulkiness of the discrete inductors has been a disadvantage for use in portable electronic devices, and hence inductors that incorporate magnetic films to boost inductance densities have researched recently [4]. The use of magnetic films shows potential for completely integrated inductors that have significantly higher inductance density and thus take up less space, ideal for portable electronics [5]. High-frequency measurements of the on-chip integrated inductors have been implemented, from which the inductance, the resistance and quality factor of the magnetic and air-core inductor can be extracted according to a two-port circuit model.

Inductors play an important role in RFICs (radio frequencies integrated circuits). This valuable distinction paves the way for researchers to work on their structures enhancement to reach optimized performance. The use of on-chip inductors for the design of integrated wireless communication systems ease the system integration and miniaturization and avoid parasite introduction. These features are, however, difficult to achieve when using discrete components.

Previous work [6] proposed solenoid inductor structures, their findings showed enhancement in the quality factor and inductance as evaluated using geometrical parameters. Recently, integrated inductors fabricated using thin films and magnetic cores [7] are developed. This design technology exhibited 10 times more performance enhancement than that of an air-core inductor of identical geometry. In this work, we proposed a new magnetic material made of FeNiCo, which can achieve optimistic permeability of 100.

In this paper, an on-chip solenoid inductor has been studied. The first part addresses, the modeling of the solenoid inductor and derivation of the relationships between geometrical parameters and the process parameters (inductance and quality factor). The second part discusses the simulation of the solenoid inductor integrated with FeNiCo. In this part, the influence of various parameters such as the operating frequency, the spacing between the coils, the number of coils, and the thickness of the magnetic core are analyzed in detail by simulation with MATLAB software. Finally, the simulation results are compared with published results of inductor designs.

2. DESIGN OF SOLENOID INDUCTOR

Figure 1 illustrates the top and cross-section views of the schematic design diagram of the solenoid rectangular micro-inductor [8]. The copper winding sets up the bottom copper tracks and the top copper tracks are connected through vias [9]. The use of magnetic cores facilitate the shape miniaturization and keeps the stray fields within limits better than air-core coil inductors. The objective of this work is to achieve a ferromagnetic resonance frequency of 4.7 GHz with the FeNiCo magnetic core as a hard axis and having a permeability of 100.

Based on the target specifications of the solenoid inductor, the design was made by adjusting parameters of the core and winding dimensions [9]. The geometrical input parameters are: the size of vias s_V, gap surrounding the vias g_V, the gap between two adjacent turns g, the thickness of coil t_C, length of coil l_C, the width of coil w_C (w_V), magnetic core thickness t_M, magnetic core width w_M, magnetic film length l_A(l_M), air-core width w_A, the thickness of the gap between top and bottom conductor t_A and number of turns N. The output parameters are the DC and AC resistance, the total inductance and maximum magnetic induction described in [10].

(a)   (b)
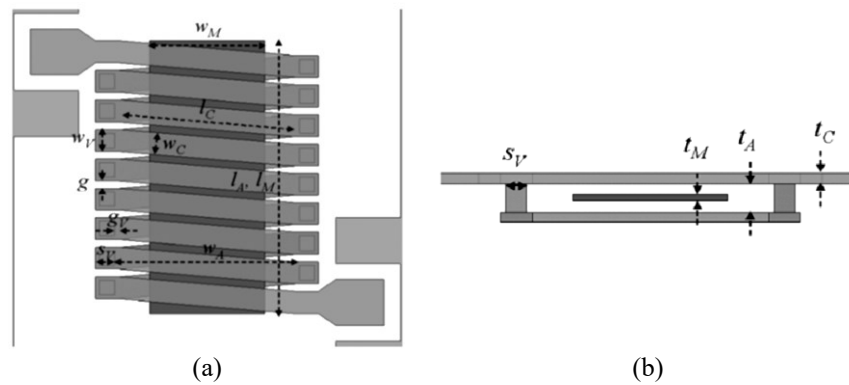
Figure 1. Schematic design of solenoid micro-inductors: (a) top view and (b) cross-section view

The relation for the inductance of the integrated solenoid inductor with air core can be expressed as:

$$L_{AC} = L_{Parasitic} + L_{Winding} \tag{1}$$

where the winding inductance $L_{Winding}$ can be described by the classical Wheeler formula [11]:

$$L_{Winding} = \frac{10.\pi.\mu_0.N^2.a^2}{9a+10l_A}, \quad a = \sqrt{\frac{(w_A+2s_V).(t_A+2t_C)}{\pi}} \tag{2}$$

The parasitic inductance $L_{Parasitic}$ describes the effects of the parasitic at the ports. If the magnetic core is included, it can be shown that the inductance [12, 13] and series resistance [14, 15] can be approximated respectively by:

$$L = \frac{\mu_0 \cdot \mu_r \cdot N^2 \cdot w_M \cdot t_M}{l_M} \tag{3}$$

$$R = \frac{2N \cdot w_M \cdot \rho_C}{w_C \cdot \delta_C \cdot (1 - e^{-(t_C/\delta_C)})} \tag{4}$$

where δ_C is the wire skin depth expressed as [16]:

$$\delta_C = \sqrt{\frac{\rho_C}{(\pi \cdot \mu_0 \cdot \mu_{rC} \cdot f)}} \tag{5}$$

where $\mu_0 = 4.\pi.10^{-7}$ [H/m] and μ_{rC} is the relative magnetic permeability of the wire. For a copper conductor case, $\mu_{rC} = 1$ and $\rho_C = 17.24 \times 10^{-9}$ [Ω.m] at 20 °C. Since the quality factor, Q, inductance, L, and resistance, R, are related as follows:

$$Q = \frac{\omega L}{R} \tag{6}$$

Hence, the quality factor can be computed by replacing (3) and (4) in (6):

$$Q = \frac{\omega \mu_0 \cdot \mu_r \cdot N \cdot t_M \cdot w_C \cdot \left(1 - e^{-(t_C/\delta_C)}\right)}{2 l_M \cdot \rho_C} \tag{7}$$

2.1. Parameter extraction

In a typical two-port circuit model shown in Figure 2, the S-parameters provide a clear physical interpretation of the transmission and reflection performance of the device [17]. It can be described in terms of the scattering parameters as:

$$\begin{bmatrix} z_1 \\ z_2 \end{bmatrix} = \begin{bmatrix} S_{11} & S_{12} \\ S_{21} & S_{22} \end{bmatrix} \cdot \begin{bmatrix} x_1 \\ x_2 \end{bmatrix} \tag{8}$$

or in terms of the admittance parameters as:

$$\begin{bmatrix} I_1 \\ I_2 \end{bmatrix} = \begin{bmatrix} Y_{11} & Y_{12} \\ Y_{21} & Y_{22} \end{bmatrix} \cdot \begin{bmatrix} V_1 \\ V_2 \end{bmatrix} \tag{9}$$

The circuit of the integrated solenoid inductor in this work is reciprocal, so $Y_{11} = Y_{22}$ and $Y_{12} = Y_{21}$. Then we have the following equations to compute the frequency dependence of the inductance and quality factor.
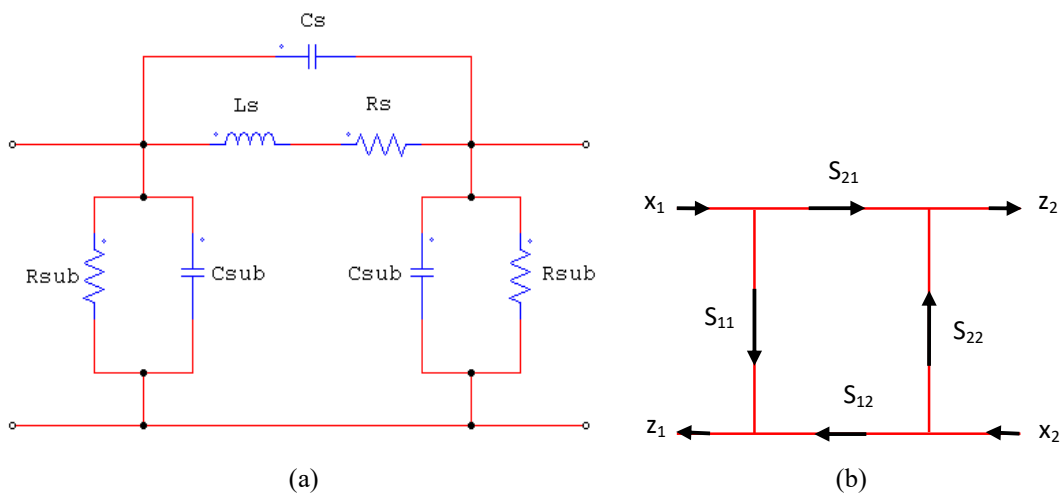
Figure 2. The equivalent circuit of
(a) the two-port model for inductors and (b) its network of S-parameters.

$$L = \frac{Im\left(\frac{1}{-Y_{12}}\right)}{2\pi f} \quad (10)$$

$$Q = -\frac{Im\left(\frac{1}{Y_{12}}\right)}{Re\left(\frac{1}{Y_{12}}\right)} \quad (11)$$

3. RESULTS AND DISCUSSION
3.1. Influence of the number of turns
Results of inductance and quality factor variation versus frequency for three different numbers of turns are shown in Figure 3. As shown in Figure 3 (a), an increase in turns number leads to an increase of inductance from 15 to 24 nH at a frequency of 1.5 GHz. However, Figure 3 (b) shows that solenoid inductor with a lower number of turns has the highest quality factor. This is because the increase of N enlarges the total length and reduces the cross-section of the coil [18].
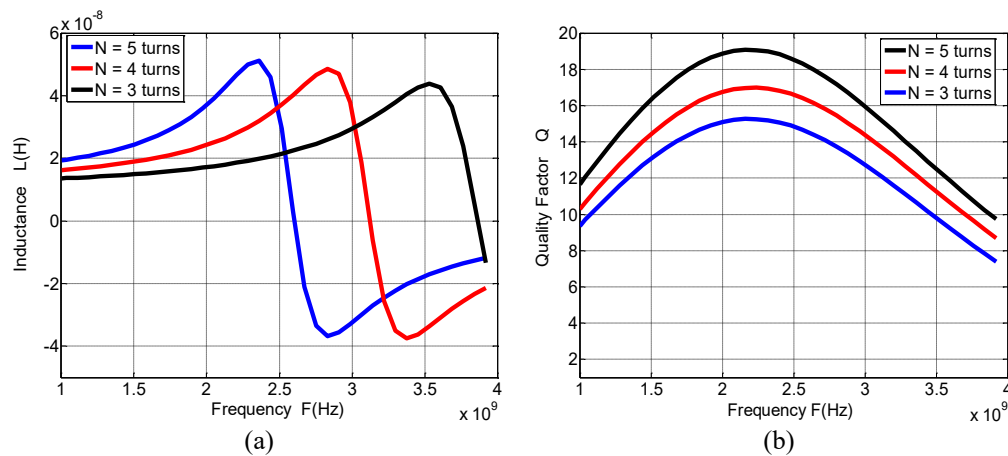
Figure 3. Illustrate (a) the inductance and (b) the quality factor versus frequency
for three different numbers of turns

3.2. Influence of the magnetic core length
Figure 4 shows the plots of the inductance and quality factor versus frequency for three different lengths of the magnetic core, which are 300, 400 and 500 μm. As shown in Figure 4 (a), the inductance decreases for high length. However, as illustrated in Figure 4 (b), the quality factor trend is the opposite for high length. This can be explained by the fact an increase in magnetic core length with turn number and gap between the two neighboring windings unchanged, results in the wider winding. This latter will lead to a lower resistance loss and hence to higher quality factor [19].

3.3. Influence of the magnetic core width
Figure 5 illustrates the inductance and quality factor as a function of the frequency for two different widths of the magnetic core, which are 310 and 420μm. The inductance increases from 15 to 21 nH at a frequency of 1.5 GHz for an increased width, while the quality factor is not too much influenced by changes in the width. Ideally, with a stable number of turn and the same gap between the two adjoining coils, the enlarged magnetic core width results in longer coils, leading to a higher resistance loss and diminish quality factor [20].

3.4. Influence of the gap between turns
Figure 6 shows the plots of quality factor and inductance variation versus frequency for gaps between the neighboring winding equal to 20μm and 15μm. The results show that an increase of about 33% of the gap did not lead to significant changes. In this simulation, we only observed a 16% increase in the inductance and a 7 % decrease in the peak quality factor at a frequency of about 2.3 GHz. This result also illustrates that an increase in the gap between the neighboring windings with a fixed magnetic core length reduces the width of windings, which leads to an increase in resistance loss [21].
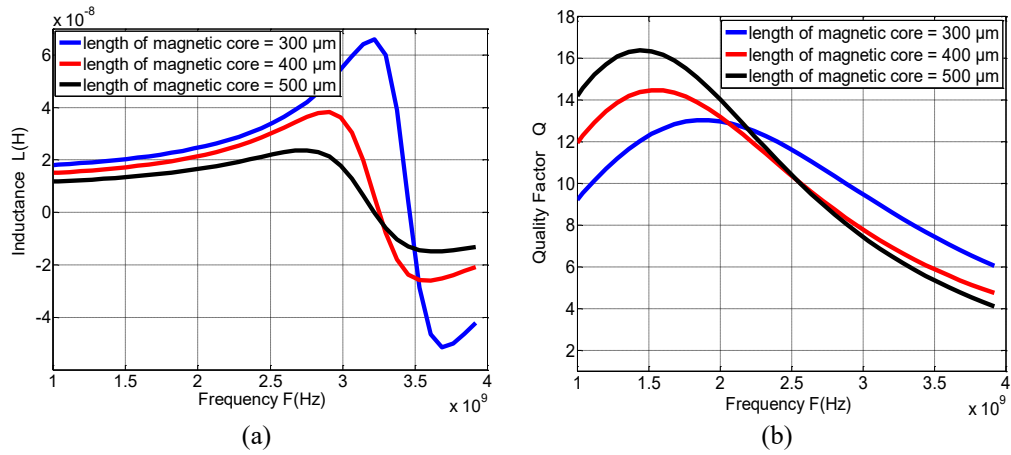
Figure 4. Illustrate (a) the inductance and (b) the quality factor versus frequency
for three different lengths of magnetic core
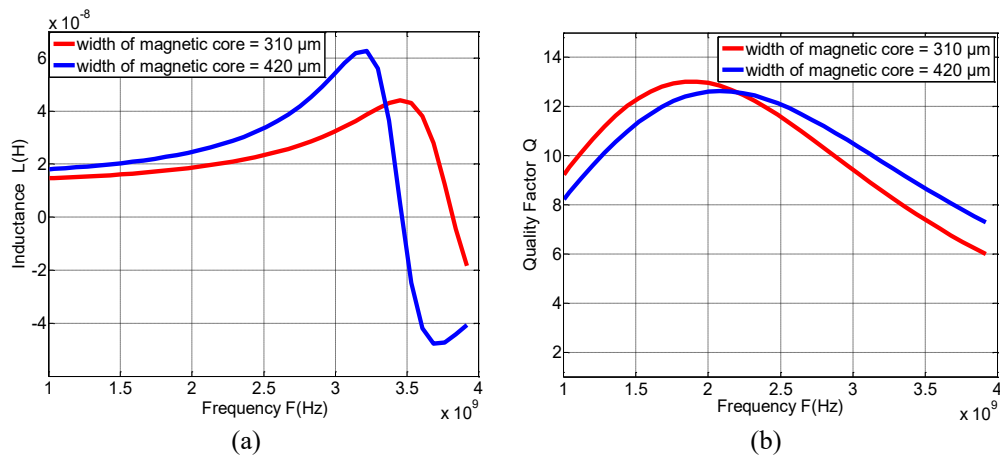
Figure 5. Illustrate (a) the inductance and (b) the quality factor versus frequency
for two different widths of magnetic core
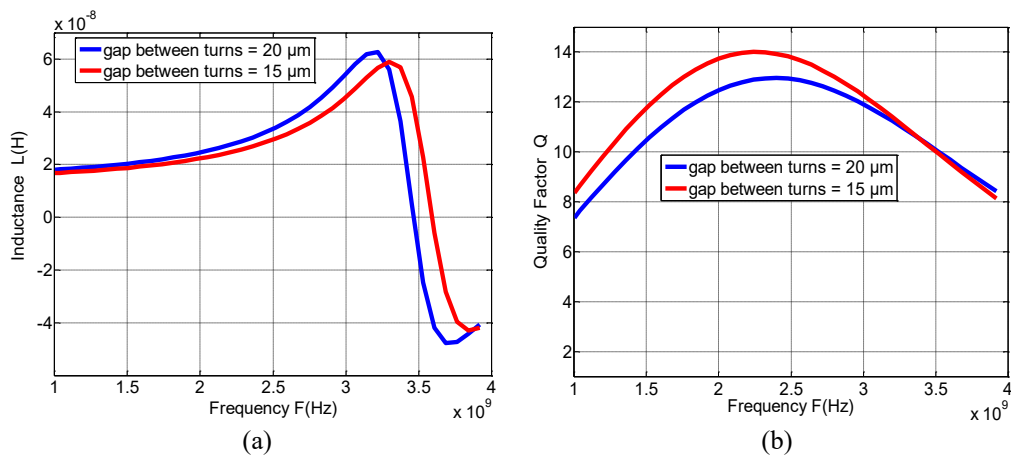
Figure 6. Illustrate (a) the inductance and (b) the quality factor versus frequency
for two different gaps between turns.

3.5. Influence of the thickness of the magnetic core

Figure 7 displays the inductance and quality factor of the solenoid inductor for two different thicknesses of the magnetic core. The results show that by increasing the thickness of the magnetic core from 1µm to 2µm improves both the inductance value and quality factor.
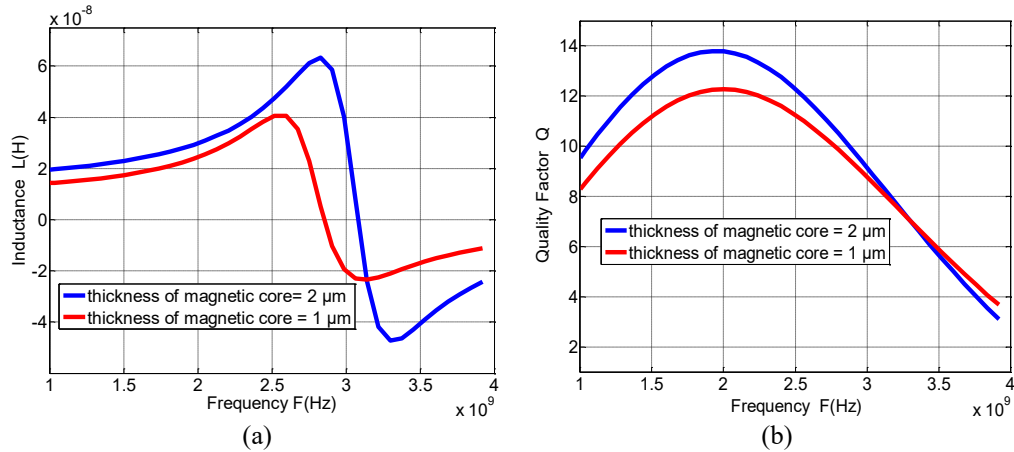
Figure 7. Illustrate (a) the inductance and (b) the quality factor versus frequency
for two different thickness of the magnetic core

3.6. Influence of the thickness of the coil

Figure 8 shows the inductance and quality factor plotted over a range of frequencies for three different thicknesses of the coils (i.e.2µm–3µm–4µm). As shown in Figure 8 (a), the inductance value for the thicker coil is more to that of the thinner coil. It can be noticed from Figure 8 (b) that the peak of the quality factor has also improved with an increase in the thickness of the coils.
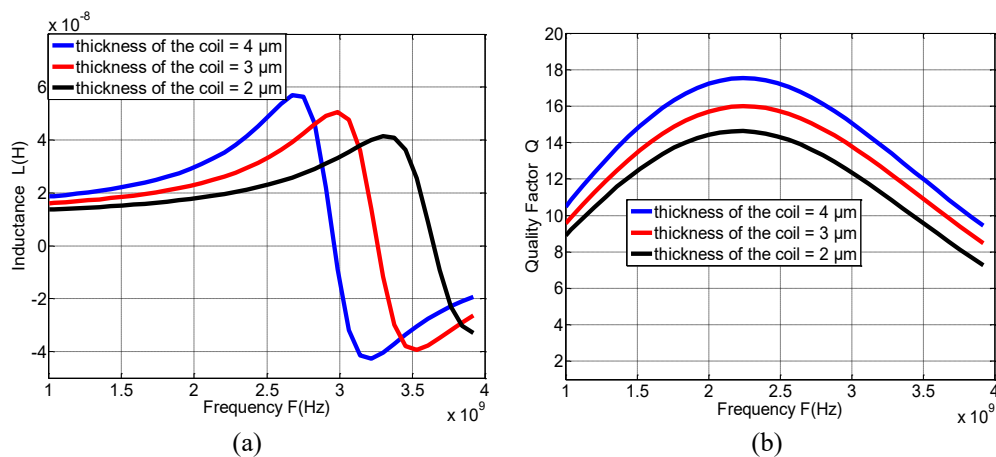
Figure 8. Illustrate (a) the inductance and (b) the quality factor versus frequency
for three different thicknesses of coils

3.7. Influence of the insulator thickness

The effect of the oxide thickness on the inductance is shown in Figure 9 (a). The enhanced silicon dioxide structure shows a boosted inductance value compared with that of conventional silicon dioxide at about 3 MHz frequency. Figure 9 (b) illustrates that the quality factor exhibits larger values with oxide thickness. This latter occurs because structure with thicker silicon dioxide layer will exhibit less loss.
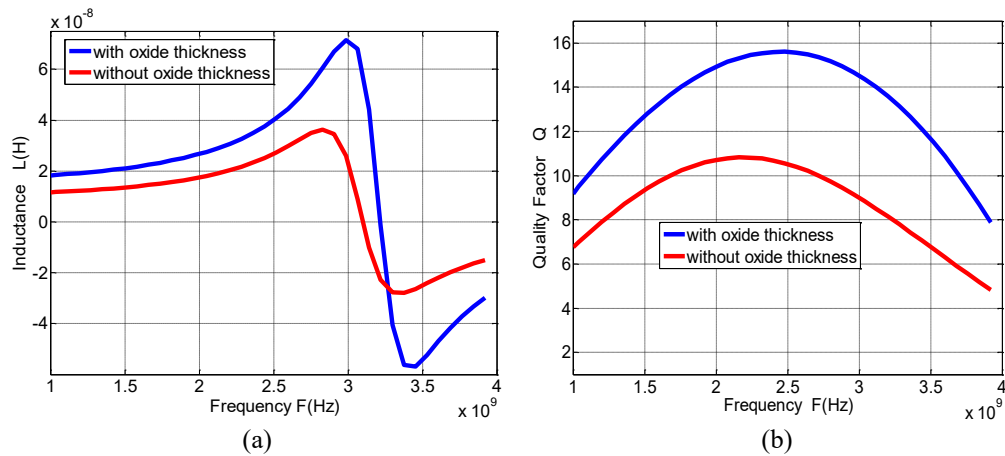
Figure 9. Illustrate (a) the inductance and (b) the quality factor versus frequency
with and without oxide thickness

3.8. Comparison of solenoid inductor with other inductors

The performance of the solenoid inductor is compared with other inductors integrated with magnetic cores as indicated in Table 1. The values mentioned in the table under 'this work' are the maximum inductance, maximum quality factor, self-resonant frequency and different magnetic materials obtained by the parametric analysis. The results show that with our design proposal, we can achieve simultaneously satisfactory enhanced inductance and quality factors at GHz frequencies.

Table 1. Comparison of integrated solenoid inductor characteristic
between 'this work' and other published results.

Inductor designs	Magnetic Materials	Frequency (Hz)	L (nH)	Qmax	Ref
Solenoid	CoTaZr	$10 .10^6$	219	4	[22]
Solenoid	$FeCoB/Al_2O_3$ Multilayer	50.10^6	13	8	[23, 24]
Solenoid On PCB	CoFeHfO	200.10^6	1	23	[25]
Solenoid	$FeGaB/Al_2O_3$ Multilayer	1200.10^6	15	20	[26]
Solenoid	FeNiCo	$(1 - 4).10^9$	20	17	This work

4. CONCLUSION

In this paper, we have presented the design and modeling of a solenoid inductor. The most challenging task encountered is to determine the appropriate electrical parameters (i.e. inductance and quality factor). Next, the optimization of the quality factor of a solenoid inductor integrated with FeNiCo requires a weakly width of the magnetic core, the gap between turns and strong numbers of turns, length of the magnetic core, the thickness of the magnetic core, the thickness of the coil and oxide thickness. Our results demonstrate cutting-edge high-frequency (one–four GHz) performance for a combination of high-quality factors and inductance values. We conclude from the results obtained in this work, that there is still a possibility to improve existing inductor structure to realize stable and better results over a wide high-frequency range. We conclude also that use of inductor simulation to analyze and understand factors that affect system parameters (i.e. quality factor and inductance) and compare them with expected desired results is pre-requisite before the design of more robust inductor.

REFERENCES

[1] Hu A., Ren Z., Zhang K., Liu L., Chen X., Liu D., Zou X., "Low-phase-noise wideband VCO with an optimized sub-nH inductor," *Electronics Letters*, vol. 51, no. 15, pp. 1209-1211, 2015.
[2] Ourak L., Ghannam A., Bourrier D., Viallon C., Parra T., "Solenoidal transformers for magnetic materials integration," *Proceedings Microwave Conference (APMC),* pp. 854-856, 2012.
[3] Benhadda Y., Hamid A., Lebey T., Allaoui A., Derkaoui M., Melati R., "Thermal Behavior of an Integrated Square Spiral Micro Coil," *TELKOMNIKA Telecommunication Computing Electronics and Control*, vol. 14, no. 2, pp. 250-265, 2015.

[4] Derkaoui M., Hamid A., Lebey T., Melati R., "Design and Modeling of an Integrated Micro-Transformer in a Flyback Converter," *TELKOMNIKA Telecommunication Computing Electronics and Control*, vol. 11, no. 4, pp. 669-682, 2013.

[5] Namoune A., Hamid A., Taleb R., "The Performance of the Transformer for an Isolated DC/DC Converter," *TELKOMNIKA Telecommunication Computing Electronics and Control*, vol. 15, no. 3, pp. 1031-1039, 2017.

[6] Liu W. Y., Suryanarayanan J., Nath J., Mohammadi S., Katehi L. P. B., Steer M. B., "Toroidal Inductors for Radio-Frequency Integrated Circuits," *IEEE Trans. Microwave Theory and Techniques*, vol. 52, no. 2, pp. 646-654, 2004.

[7] Lee W. D., Hwang K. P., Shan X. W., "Fabrication and Analysis of High-Performance Integrated Solenoid Inductor with Magnetic Core," *IEEE Transactions on Magnetics*, vol. 44, no. 11, pp. 4089-4095, 2008.

[8] Gardner D., Gerhard Schrom S., Paillet F., Jamieson B., Karnik T., Borkar S., "Review of On-Chip Inductor Structures with Magnetic Films," *IEEE Transactions on Magnetics*, vol. 45, no. 10, pp. 4760-4766, 2009.

[9] Zhuang Y., Vroubel M., Rejaei B., Burghartz J. N., "Integrated RF inductors with micro-patterned NiFe core," *Solid-State Electronics*, vol. 51, no. 3, pp. 405-413, 2007.

[10] Homnawang N., "Surface Micromachined Arch-Shape On-Chip 3-D Solenoid Inductors for High-frequency applications," *Journal of Micro Nanolithography*, vol. 2, no. 4, pp. 275-281, 2003.

[11] Lee T. H., "The Design of CMOS Radio-Frequency Integrated Circuits," 2nd Ed. Cambridge University Press, New York, 2004.

[12] Lei C., "Fabrication of a solenoid-type inductor with Fe-based soft magnetic core," *J. Magn. Magn. Mater.*, vol. 308, no. 2, pp. 284-288, 2007.

[13] Gardner D., Schrom G., Paillet F., Jamieson B., Karnik T., Borkar S., "Review of on-chip inductor structures with magnetic films," *IEEE Trans. Magn.*, vol. 45, no. 10, pp. 4760-4766, 2009.

[14] Golmakani A., Mafizejad K., Razzaghpour M., Kouzani A., "Modeling and optimization of a solenoidal integrated inductor for RF Ics," *International Journal of RF and Microwave Computer-Aided Engineering*, vol. 20, no. 2, pp. 182-189, 2010.

[15] Tai C. M., Liao C. N., Nat T. H., Hsinchu U., "A Physical Model of Solenoid Inductors on Silicon Substrates," *IEEE Transaction on Microwave Theory and Technique*, vol. 55, no. 12, pp. 2579-2585, 2007.

[16] Yook J. M., "High-quality solenoid inductor using dielectric film for multichip modules," *IEEE Transactions Microwave Theory and Techniques*, vol. 53, no. 6, pp. 2230-2234, 2005.

[17] Grandi G., Kazimierczuk M. K., Massarini A., Reggiani U., Sancineto G., "Model of Laminated Iron-Core Inductors for High Frequencies," *IEEE Transactions on Magnetics*, vol. 40, no. 4, pp. 1839-1845, 2004.

[18] Flynn D., Sudan N. S., Toon A., Desmulliez M. P. Y., "Fabrication process of a micro inductor utilizing a magnetic thin film core," *Microsyst. Technol.*, vol. 12, no. 10–11, pp. 923-933, 2006.

[19] Frommberger M., et al. "Integration of crossed anisotropy magnetic core into toroidal thin-film inductors," *IEEE Trans. Microw. Theory Tech.*, vol. 53, no. 6, pp. 2096-2100, 2005.

[20] Fang D. M., Wang X. N., Zhou Y., Zhao X. L., Fabrication and performance of a micromachined 3-D solenoid inductor," *J. Microelectron.*, vol. 37, no. 9, pp. 948-951, 2006.

[21] Gu L., Li X., "High-Q Solenoid Inductors with a CMOS-Compatible Concave-Suspending MEMS Process," *Journal of Microelectromechanical Systems*, vol. 16, no. 5, pp. 1162-1172, 2007.

[22] Wu H., Gardner D. S., Xu W., Yu H. B., Integrated RF On-Chip inductors with patterned Co-Zr-Ta-B films," *IEEE Transactions on Magnetics*, vol. 48, no. 11, pp. 4123-4126, 2012.

[23] Xing X., et al. "RF magnetic properties of FeCoB/Al$_2$O$_3$/FeCoB structure with varied Al$_2$O$_3$ thickness," *IEEE Transactions on Magnetics*, vol. 47, no. 10, pp. 3104-3107, 2011.

[24] Xing X., Sun N, X., Chen B. X., "High-bandwidth low-insertion loss solenoid transformers using FeCoB multilayers," *IEEE Transactions on Power Electronics*, vol. 28, no. 9, pp. 4395-4401, 2013.

[25] Li L. L., "Small-resistance and high-quality-factor magnetic integrated inductors on PCB," *IEEE Transactions on Advanced Packaging*, vol. 32, no. 4, pp. 780-787, 2009.

[26] Gao Y., Zare S., Yang X., Nan T. X., Zhou Z. Y., Onabajo M., Liu M., Aronow A., Mahalingam K., Howe B. M., Brown G. J., Sun N. X., "Significantly enhanced inductance and quality factor of GHz integrated magnetic solenoid inductors with FeGaB/Al2O3 multilayer films," *IEEE Transactions on Electron Devices*, vol. 61, no. 2, pp. 1470-1476, 2014.